Chapter 4

Tungsten trioxide thin film: characterisation and application in asymmetric nematic liquid crystal cells.

4.1 Preface

The first material inserted in nematic liquid crystal (NLC) cells was the tungsten trioxide (WO_3) [1, 2], the most used active electrochromic oxide. A quantitative model has been developed [4] to explain the interaction between the WO_3 oxide film and the liquid crystal by the formation of charged layers at the interface, giving rise to a reverse internal electric field, which counteracts the reorientation of NLC molecules (Freedericksz transition). In this case the effect can be ascribed to mobile protons always present in these films [5]. To have further confirmations of the model and a better understanding of the basic mechanism underlying the rectification effect and the connections with the structural

and electrical properties of the films, WO_3 layers have been studied before and after thermal treatement.

4.2 Sol-gel synthesis of WO_3

The ITO-coated glasses used as substrates were ultrasonically cleaned in acetone, then in bidistilled water and finally in isopropanol and then drying with warm air [9].

Tungsten trioxide sol-gel route is reported in ref. [10-11]. Briefly, $WOCl_4$ was dissolved in dry isopropanol in Glove Box; with concentration of water and oxygen less than 0.1ppm and after stirring for one night the solution was used for coating [12].

Different spinning rate, between 600 and 7800 rpm have been tested for coating and here is reported the analysis done on the films obtained at 1200 rpm.

4.3 Raman spectroscopy

The thin film of tungsten oxide obtained by spin coating constitute an amorphous layer, containing water molecules coming from the moisture of the

air during and after spin-coating deposition. The annealing at 100 °C and 300 °C induce some water loss, but the structure is basically unchanged while the highest temperature annealing, at 600 °C, on the contrary, induces remarkable change in the films structure, revealed even by microscopic observation, as clearly reported in Fig.1.
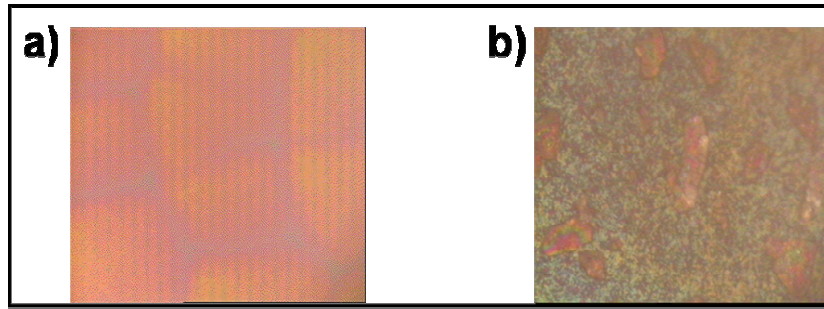

Fig.1) Optical image of the Tungsten oxide film a) not annealed b) annealed at 600°C.

The Raman cross section of such films, "as deposited" or after moderate thermal treatments, must be quite low so that, no appreciable signal can be detected in reasonable times. On the other hand, for the films annealed at 600 °C, the Raman spectra show very sharp peaks at 975, 928, 812 and 312 cm^{-1}, and weaker bands at 302 and 622 cm^{-1}, indicating well crystallized structures (see Fig. 4): a

92

more detailed discussion of these data will be reported elsewhere; it is worth, within the aims of the present work to remark the occurrence of a crystallization process (see fig.2).
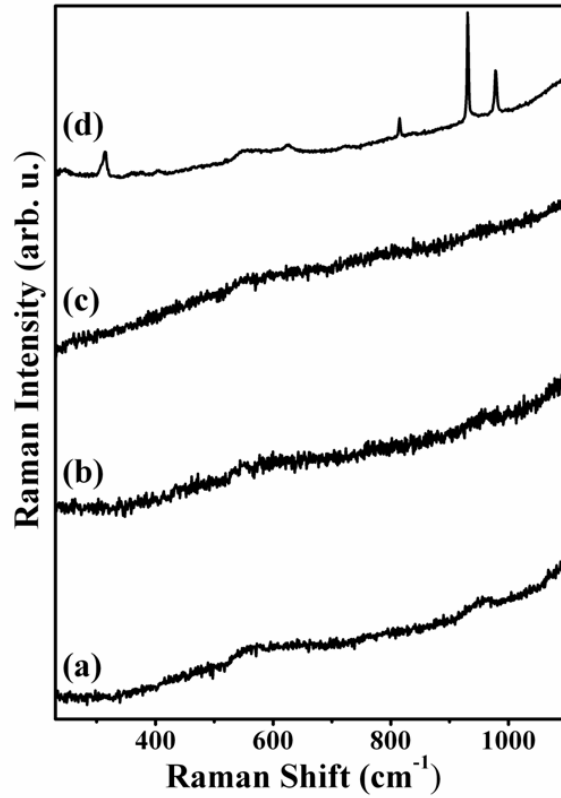

Fig.2) Raman spectra collected on Tungsten Oxide samples (a) not annealed, (b) annealed at 100°C, (c) annealed a 300°C and (d and e) annealed at 600°C.

4.4 Electrooptical response

Asymmetric NLC cell, assembled as described above, have been tested to monitor the evolution of the electrooptic response as a function of the thermal treatment of the inserted tungsten trioxide layer (Fig.5).

The most interesting fact is the decrease of the rectification effect on the electrooptic response of the cell when the WO_3 film was previously annealed at 300 °C, while a full recovery of the effect is observed for film undergoing a higher temperature annealing at 600 °C, but the sign of the effect is inverted. The inhibition of the optical switching of NLC layer occurs for the anodic polarization of the WO_3 -coated electrode in the case of "as deposited" or moderately annealed films, confirming the results previously observed [1,2] on similar cells containing WO_3 films deposited by magnetron sputtering; on the contrary, the same inhibition of the switching, associated to the maximum transmittance of light between the crossed polarizers, occurs during the phase of cathodic polarization of the plate electrode annealed at the highest temperature, suggesting the hypothesis of a change of sign of the dominant

94

charge carriers. As clearly observed in Fig.5, the rectified square wave response is very neat in the two extreme cases (see Figs. 3a and 3c), while it is partial and overlapped to a non- rectified, impulsive response, typical of the usual symmetric cells, for the intermediate annealing case (see Fig 3b).This behaviour suggests that a decrease of charge carriers number or conductivity occurs in such case for the films, without great associated structural transformation, as suggested by the vibrational spectroscopy data.
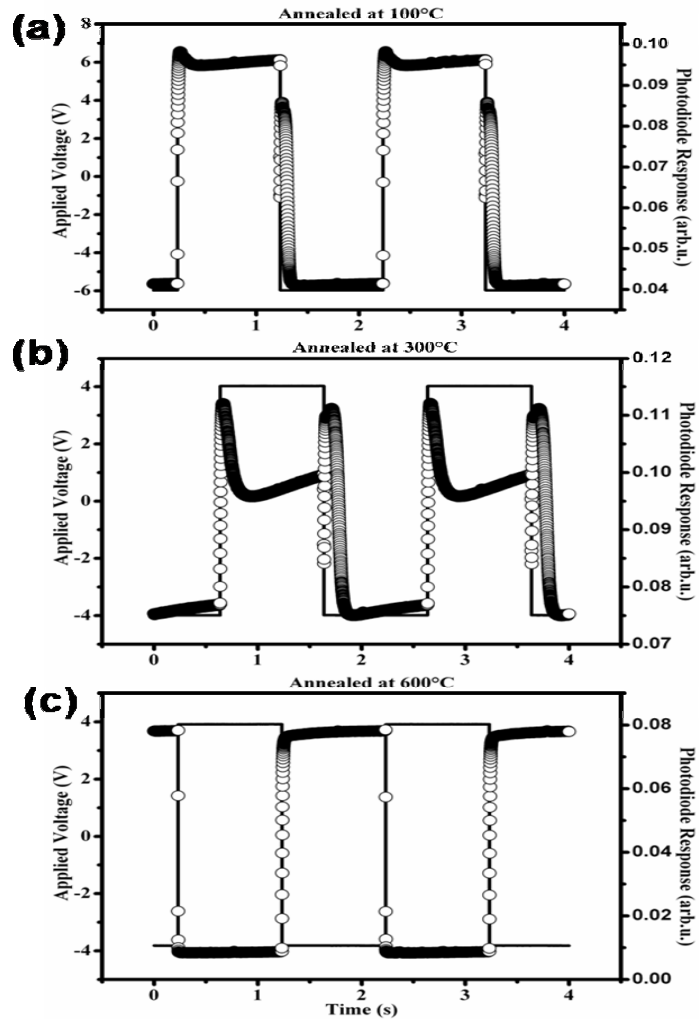
Fig. 3) Photodiode Response (open circle) of NLC Cells with inserted as electrode WO$_3$ films, annealed at 100°C (a), at 300°C (b) and at 600°C (c). The solid line is the applied voltage.

4.5 Impedance spectroscopy

Direct measurements of the thin film impedance give a rough confirmation about the change of conductivity of the films, as a function of the annealing temperature. Even taking into account the difficulty of comparison for absolute conductivity value between different samples, it is clear that an appreciable decrease of electric conductivity occurs for the films undergoing intermediate treatment at 300 °C, as it can be seen from the Bode plot of real part of impedance reported in Fig.4 for three typical films.
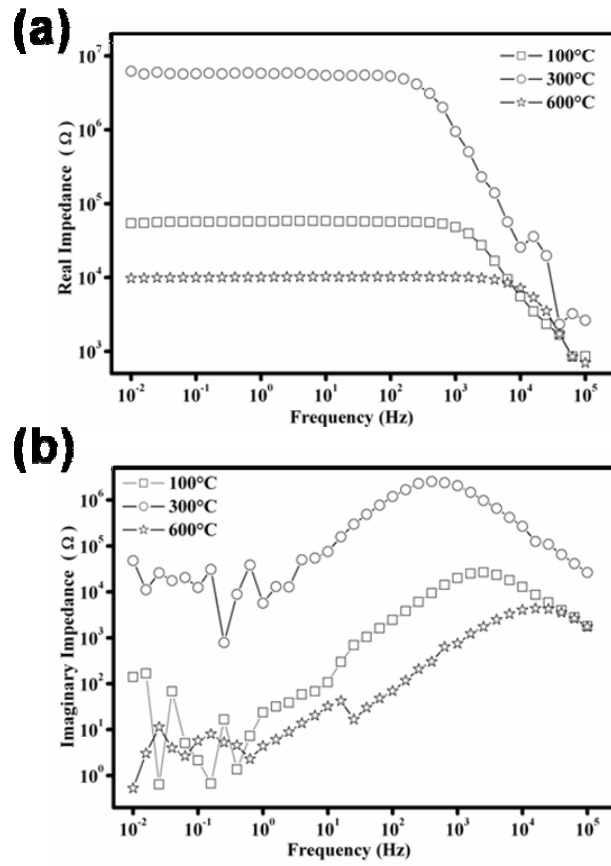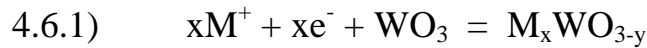
Fig. 4) Real part (a) and imaginary part (b) of the impedance of the tungsten oxide films annealed at different temperature.

4.6 Theoretical model

WO_3 is an electrochromic material that can accept a large amount of cations (K^+, Na^+, Li^+, H^+) from a source to form nonstoichiometric tungsten bronze according to the reaction

4.6.1) $xM^+ + xe^- + WO_3 = M_xWO_{3-y}$

were M^+ are the cations and $0 \leq x \leq 0.5$ and $0 \leq y \leq 0.3$ [13].

Let us first analyse the ITO-WO_3 interface alone. ITO has free electrons. They can diffuse into WO_3 pores were they force hydrogen to be bound by WO_3, forming regions of H_xWO_3 bronze. The ITO side of the interface remains positively charged whereas the WO_3 side of it remains with an unbalanced negative (localized OH^-) charge. The total (and local) concentration of H^+ has diminished so the reaction $H_2O \leftrightarrow H^+ + OH^-$ can proceed until the electric field from ITO toward WO_3 can now block the diffusion of electrons. A contact potential sets in. Connecting the two faces electrically, a current will flow, delivering electrons to the ITO

side of WO_3, until all the water and/or the catalyst sites are used.

If the ITO side is positively charged the protons in WO_3 are pushed to the right leaving an increasing negative charge to the left. In the meantime a lack of protons on the left side of WO_3 causes Eq.(4.6.1) to go from left to right, creating an increased number of protons, which are pushed to the right. Hence, the total positive charge on the right side of WO_3 layer becomes larger. If we consider n the concentration of negative charges which does not vary and $n(z)$ the concentration of positive ions, there is a net negative charge q where $n(z)<n$, and there is an equal positive charge of the same magnitude where $n(z)>n$. A plot of positive and negative charge carriers concentration across the WO_3 layer is shown in fig. 4.6.1.
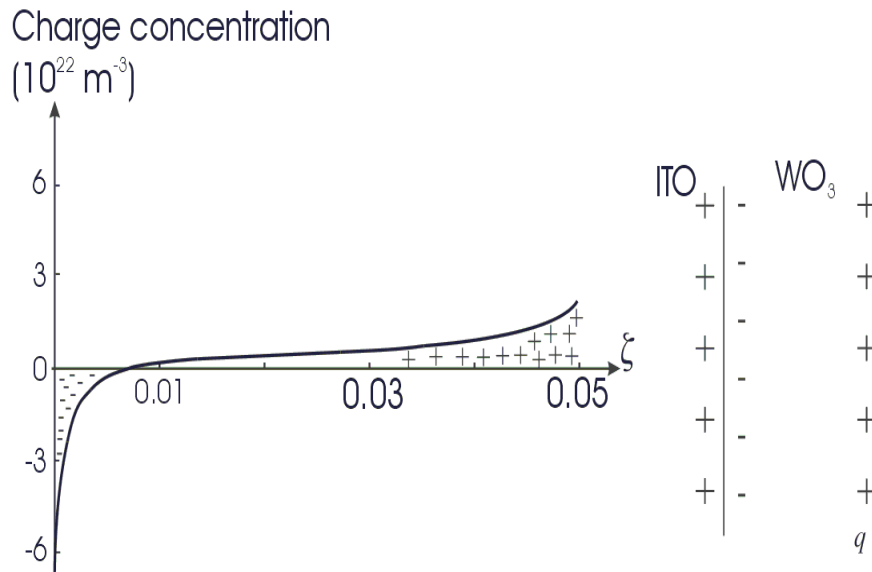
Fig. 4.6.1) Charge concentration of protons in WO₃ with anodic polarisation

If now the ITO is negatively charged, the protons are pulled to the left where they combine with a flux of ITO electrons. The stored charge are reversed but the new value q' is less than q due to hydrogen bronze formation (see fig. 4.6.2). these two mechanism, intercalation and deintercalation of protons at the left side of the WO₃ film, of which the latter seems to bee more important, can explain quite easily why the discharge current following anodic polarisation was larger than the discharge

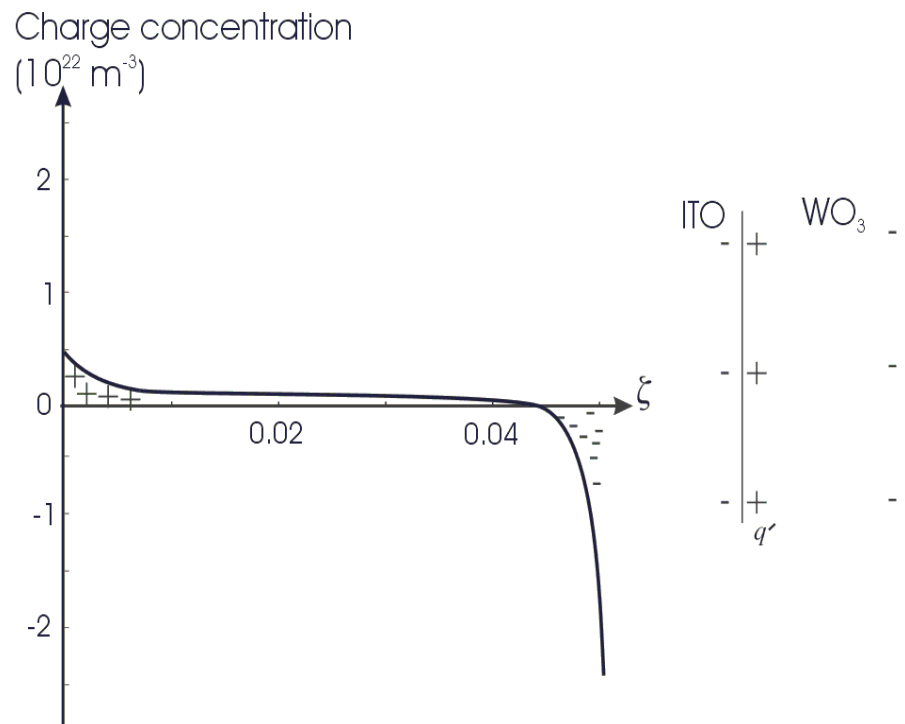current that followed the cathodic polarisation, i.e., the stored charge are different.

fig. 4.6.2) Charge concentration of protons in WO₃ with cathodic polarisation. The absolute value is about three time smaller than in fig. 4.6.1.

Now we have to take into account the role played by the liquid crystal. If the liquid crystal were a perfect dielectric, when applying an electric voltage

across the cell the potential would vary linearly with the distance and the electric field would be constant. In contrast, if the liquid crystal contains a certain amount of free ions, there will be a build up of negative charge on the anodic side of the cell and a similar build up of positive charge on the other side. The electric potential will no longer have a linear dependence and the electric field will no be constant. It will present a lower value in the bulk of the liquid crystal layer and higher value close to the surfaces. In figure 4.6.3 are showed the graphics of the potential and electric field into the liquid crystal for both anodic and cathodic polarisation of the oxide. The difference between the two cases is due to the different net charge q and q' accumulated to the WO_3-LC interface, consequently the electric field in the bulk of liquid crystal is over the Frederiks threshold only during the cathodic polarisation.
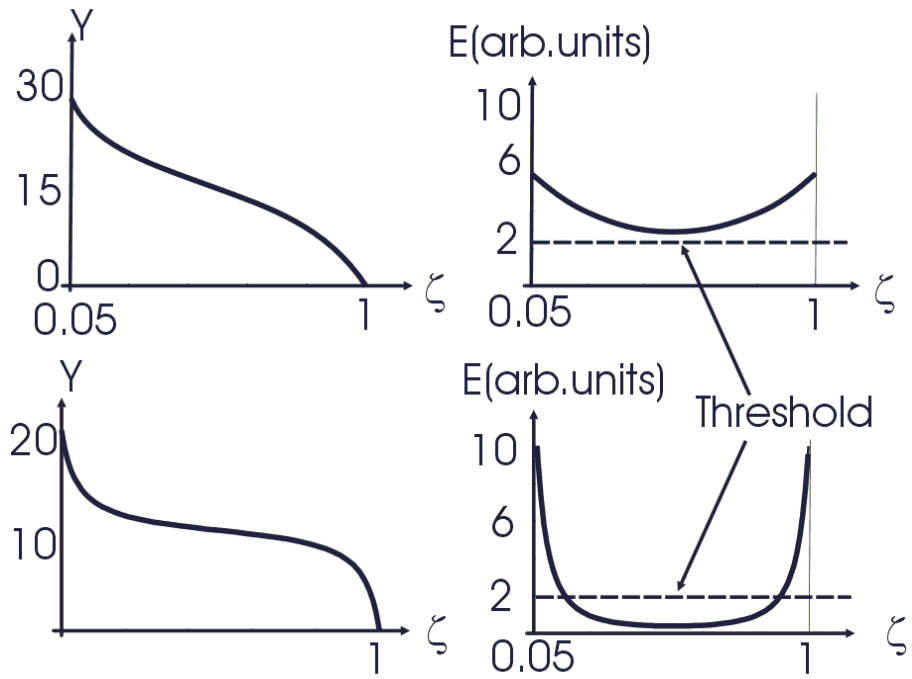
Fig. 4.6.3) The trend of the electric potential in liquid crystal region (left) and the electric field (right) for the two cases of polarisation, anodic (down) cathodic (up). For a better comparison the algebraic sign was disregarded.

The graphics in figure 4.6.3 has been obtained starting from the chemical potential

$$\mu = eV(z) + kT \ln n(z) \qquad 4.6.2)$$

where $n(z)$ is the concentration of positive ions and $V(z)$ is the electric potential experienced by the protons inside WO_3. From the equilibrium requirement that the chemical potential be uniform throughout the distribution of positive ions, we get

$$n(z) = n(\bar{z}) \exp\left(-\frac{e[V(z) - V(\bar{z})]}{kT}\right) = n(\bar{z}) \exp[-\Psi(z)] \qquad 4.6.3)$$

where, for $z \in [0, d]$, we use an adimensional potential $\Psi_1(z) = eV(z)/kT$. Let $\Psi_1(0) = \Psi_0$, the potential of ITO-WO_3 interface. We speak of anodic case if $\Psi_0 > 0$ and of cathodic case if $\Psi_0 < 0$. The other contact (liquid crystal-ITO interface) is grounded. Consequently

$$\Psi_1(\bar{z}) = \frac{eV(\bar{z})}{kT}, \ \Psi(z) = \Psi_1(z) - \Psi_1(\bar{z}), \ \Psi(\bar{z}) = 0 \qquad 4.6.4)$$

if n is the constant concentration of negative chrge (OH^-), we should choose $\bar{z}$ as the root of the equation $n(z) = n$, i.e., the surface between the WO_3 layer where the net charge density is zero. Considering that the entire layer of WO_3 does not

have any net charge, the following condition has to be fulfilled:

$$n \; d = \int_0^d n(z)dz = n(\bar{z})\int_0^d \exp[-\Psi(z)]dz \quad 4.6.5)$$

or

$$\frac{1}{d}\int_0^d \exp[-\Psi(z)]dz = 1$$

One further important fundamental equation will be required. This is the well known Poisson equation

$$-\varepsilon_0\varepsilon_1\frac{d^2V(z)}{dz^2} = e[n(z)-n] \qquad 4.6.6)$$

or

$$\frac{d^2\Psi(z)}{dz^2} = -\frac{e^2n}{\varepsilon_0\varepsilon_1 kT}\{\exp[-\Psi(z)]-1\} \qquad 4.6.7)$$

It is convenient to use a new adimensional coordinate

$$\xi = \frac{z}{D} \qquad\qquad 4.6.8)$$

where D is the total thickness of the cell (including the thickness d of the WO$_3$ layer). Let

$$\delta = \frac{d}{D}, \quad L_1^2 = \frac{\varepsilon_0 \varepsilon_1 kT}{2ne^2} \qquad\qquad 4.6.9)$$

Equation 4.6.7 become

$$\frac{d^2\Psi(\zeta)}{d\zeta^2} = -\frac{D^2}{2L_1^2}\{\exp[-\Psi(\zeta)]-1\} \qquad 4.6.10)$$

where $L_1 = \sqrt{\varepsilon_0 \varepsilon_1 kT / 2ne^2}$ is the so called Debye screening length ε_1, is the dielectric constant of the WO$_3$ and e $= +1.6 * 10^{-9}$ C. the dielectric constant ε_1 is typically about 6; it may depend on the porosity of the WO$_3$ layer. This values does not

take into account the mobile charge of the liquid crystal and the protons of the WO_3. In other words, ε_1 is the dielectric constant of a pure matrix of WO_3 free of charges. The equation 4.6.5 become

$$\frac{1}{\delta}\int_0^\delta \exp[-\Psi(\zeta)]d\zeta = 1 \qquad 4.6.11)$$

It can easily proved that equation 4.6.9 is equivalent to

$$\left(\frac{d\Psi}{d\zeta}\right)^2 = \frac{D^2}{L_1^2}[\exp[-\Psi(\zeta)] + \Psi(\zeta) + c] \quad 4.6.12)$$

or

$$\frac{d\Psi(\zeta)}{d\zeta} = \pm a\sqrt{\exp[-\Psi(\zeta)] + \Psi(\zeta) + c} \quad 4.6.13)$$

where the negative sign is associate to the anodic polarisation ($\Psi_0 > 0$) and the positive sign to the cathodic polarisation ($\Psi_0 < 0$). Also

$$a = \frac{D}{L_1} \qquad 4.6.14)$$

and the integration constant c should be greater than -1. Let us now use the condition 4.6.9

$$\frac{1}{\delta}\int_0^\delta \exp[-\Psi(\zeta)]d\zeta = -\frac{2}{a^2\delta}\int_0^\delta \frac{d^2\Psi(\zeta)}{d\zeta^2}d\zeta + 1 = 1 \quad 4.6.15)$$

that is

$$\int_0^\delta d\left(\frac{d\Psi(\zeta)}{d\zeta}\right) = 0 \Rightarrow \left.\frac{d\Psi(\zeta)}{d\zeta}\right|_0 = \left.\frac{d\Psi(\zeta)}{d\zeta}\right|_\delta \quad 4.6.16)$$

using now equation 4.6.12, one gets

$$\exp[-\Psi(\delta)] + \Psi(\delta) = \exp[-\Psi(0)] + \Psi(0) \quad 4.6.17)$$

Remembering expression 4.6.4 one has

$$\Psi_1(0) = \Psi_0 = \Psi_1(\overline{\zeta}) + \Psi(0)$$

and

$$\Psi_1(\delta) = \Psi_1(\overline{\zeta}) + \Psi(\delta) = \Psi_0 + \Psi(\delta) - \Psi(0)$$

or

$$\Psi(\delta) = \Psi_1(\delta) - \Psi_0 + \Psi(0) \qquad 4.6.18)$$

the equation 4.6.16 become

$$\exp[\Psi_0 - \Psi_1(\delta)]\exp[-\Psi(0)] + [\Psi_1(\delta) - \Psi_0] + \Psi(0)$$
$$= \exp[-\Psi(0)] + \Psi(0)$$

or

$$\Psi_1(\delta) - \Psi_0 = e^{-\Psi(0)}\left[1 - e^{[\Psi_0 - \Psi_1(\delta)]}\right]$$

i.e.,

$$\Psi(0) = \ln\left[\frac{e^{[\Psi_0 - \Psi_1(\delta)]} - 1}{\Psi_0 - \Psi_1(\delta)}\right] \qquad 4.6.19)$$

let us now integrate the equation 4.6.12

$$\int_{\Psi(0)}^{\Psi(\zeta)} \frac{d\phi}{\sqrt{\exp(-\phi) + \phi + c}} = \mp a\int_0^{\zeta} d\zeta = \mp a\zeta \qquad 4.6.20)$$

For $\zeta = \delta$ the previous expression become

$$\int_{\Psi(0)}^{\Psi(\delta)} \frac{d\phi}{\sqrt{\exp(-\phi) + \phi + c}} = \mp a\delta \qquad 4.6.21)$$

111

Using equations 4.6.17 and 4.6.18 $\Psi(\delta)$ can be expressed in term of $\Psi_1(\delta)$ (potential at the WO$_3$-liquid crystal interface) and Ψ_0 which is known.

$$\Psi(\delta) = \Psi_1(\delta) - \Psi_0 + \ln\left[\frac{e^{[\Psi_0 - \Psi_1(\delta)]} - 1}{\Psi(0) - \Psi_1(\delta)}\right] \quad 4.6.22)$$

The integral in equation 4.6.20 depends on the characteristic of the cell (a, δ), the applied voltage Ψ_0 and also on two unknowns $\Psi_1(\delta)$ and c. The integral can be done numerically for a set of values for $\Psi_1(\delta)$ (between 0 and Ψ_0) and for a set of values for c. The minimum value of the potential slope—i.e., $\left(\dfrac{d\Psi}{d\zeta}\right)$ occurs when $\Psi = \Psi(\overline{\zeta}) = 0$ and is $a\sqrt{1 + c}$ Therefore, $c > -1$. Moreover the minimun slop cannot be greater than $\left[\dfrac{\Psi_0 - \Psi_1(\delta)}{\delta}\right]$ which limits the values of c. Thus, one has to choose the values of c in the set $\left(-1, -1 + \dfrac{[\Psi_0 - \Psi_1(\delta)]^2}{a^2\delta^2}\right)$. A three-dimensional plot

of the numerical values of the integral in Eq. 2.6.20 with respect to $\Psi_1(\delta)$ and c represents a surface (let it be $\Sigma(\Psi_1(\delta), c)$). Intersecting it with the plane $\Sigma = a\delta$ one obtains a curve that gives a connection between c and $\Psi_1(\delta)$, namely, $c = c(\Psi_1(\delta))$. In that manner, the constant c is eliminated and only one parameter $\Psi_1(\delta)$ is left unknown. But, at the WO_3 - LC interface, disregarding any trapped charge, one can use the continuity relations

$$\Psi_1(\delta) = \Psi_2(\delta)$$

and

$$\varepsilon_1 \left.\frac{d\Psi_1(\zeta)}{d\zeta}\right|_\delta = \varepsilon_2 \left.\frac{d\Psi_2(\zeta)}{d\zeta}\right|_\delta \qquad 4.6.23)$$

which connect the potential $\Psi_1(\zeta)$ defined for $\zeta \in [0,\delta]$ with the potential $\Psi_2(\zeta)$ defined for $\zeta \in [\delta,1]$, that is in the liquid crystal region.

Coming back to the expression 4.6.19 the integral in the left hand side can also be done numerically for a set of values Ψ (limited by $\Psi(0)$ and $\Psi(\delta)$).

Representing now the set Ψ on the ordinate and corresponding values of ζ on the abscissa we get the graphic of the function $\Psi(\zeta)$. Of course, this procedure can be repeated for several values of $\Psi_1(\delta)$ and one obtain a family of curves $\Psi(\zeta)$ from which one get the family

$$\Psi_1(\zeta) = \Psi(\zeta) + \Psi(0) - \ln\left[\frac{e^{[\Psi_0 - \Psi_1(\delta)]} - 1}{\Psi_0 - \Psi_1(\delta)}\right] \quad 4.6.24)$$

We can now consider that in the liquid crystal there are positive and negative ions free to move, either as ionic impurities or as the equilibrium dissociation of liquid crystal molecules themselves. Let $n_p(\zeta)$ and $n_n(\zeta)$ be the concentrations of positive and negative ions, respectively. At equilibrium or very close to equilibrium (as the power dissipated in the sample is quite small $\cong 0.1 \mu W / cm^2$) the values of the concentration are

$$n_p(\zeta) = n_p(\bar{\zeta}) \exp\left[-\Psi_2(\zeta) + \Psi_2(\bar{\zeta})\right] \quad 4.6.25)$$

$$n_n(\zeta) = n_n(\bar{\zeta})\exp[\Psi_2(\zeta) - \Psi_2(\bar{\zeta})]$$

where

$$\Psi_2(\zeta) = \frac{eV(\zeta)}{kT} \text{ for } \delta \leq \zeta \leq 1 \text{ and } \Psi_2(1) = 0 \quad 4.6.26)$$

that is, $\Psi_2(\zeta)$ is the adimensional potential within the liquid crystal region.
It is easy to verify that the product of the concentration does not depend on ζ and may be called n_i^2 (constant),

$$n_p(\zeta)n_n(\zeta) = n_p(\bar{\zeta})n_n(\bar{\zeta}) = n_i^2 \quad 4.6.27)$$

One may recognize a well known formula in the physics of semiconductors. The values $\bar{\zeta}$ can conveniently be chosen as that values of ζ for which the two concentration are equal

$$n_p(\bar{\zeta}) = n_n(\bar{\zeta}) = n_i \quad 4.6.28)$$

In the liquid crystal zone $\delta \leq \zeta \leq 1$ where ε_2 is the dielectric constant of the liquid crystal, the Poisson equation is

$$\frac{d^2\Psi_2(\zeta)}{d\zeta^2} = -\frac{e^2 D^2}{\varepsilon_2 \varepsilon_0 kT}\left[n_p(\zeta) - n_n(\zeta)\right]$$

$$= -\frac{e^2 n_i D^2}{\varepsilon_2 \varepsilon_0 kT}\left\{\exp\left[-\Psi_2(\zeta) + \Psi_2(\bar{\varepsilon})\right] - \exp\left[\Psi_2(\zeta) - \Psi_2(\bar{\zeta})\right]\right\}$$

4.6.29)

then

$$\frac{d^2\Psi_2(\zeta)}{d\zeta^2} = \frac{D^2}{L_2^2}\operatorname{senh}\left[\Psi_2(\zeta) - \Psi_2(\bar{\zeta})\right] \quad 4.6.30)$$

where

$$L_2^2 = \frac{\varepsilon_2 \varepsilon_0 kT}{2e^2 n_i} \qquad 4.6.31)$$

L_2 play the role of the Debye length for the liquid crystal zone. Due to the symmetry of the problem in the liquid crystal region, $\bar{\zeta}$ would be the middle point, i.e., $\bar{\zeta} = \dfrac{1+\delta}{2}$ and $\Psi_2(\bar{\zeta}) = \dfrac{1}{2}\Psi_1(\delta)$. To simplify the notation, we set

$$\varphi(\zeta) = \Psi_2(\zeta) - \Psi_2(\bar{\zeta}) \qquad 4.6.32)$$

$\Psi_2(\bar{\zeta})$ and Ψ_0 being constant, we have

$$\frac{d\Psi_2(\zeta)}{d\zeta} = \frac{d\varphi(\zeta)}{d\zeta}, \ \ \frac{d^2\Psi_2(\zeta)}{d\zeta^2} = \frac{d^2\varphi(\zeta)}{d\zeta^2} \qquad 4.6.33)$$

as well as the useful expression

$$\Psi_2(\zeta) = \varphi(\zeta) + \Psi_2(\bar{\zeta}), \quad \varphi(1) = -\Psi_2(\zeta) = -\frac{1}{2}\Psi_1(\delta),$$

$$\varphi(\delta) = \frac{1}{2}\Psi_1(\delta) \qquad\qquad 4.6.34)$$

It can be seen that the equation

$$\frac{d^2\varphi(\zeta)}{d\zeta^2} = \frac{D^2}{L_2{}^2}\text{senh}[\varphi(\zeta)] \qquad 4.6.35)$$

is equivalent to

$$\left(\frac{d\varphi(\zeta)}{d\zeta}\right)^2 = \frac{2D^2}{L_2{}^2}\cosh[\varphi(\zeta)] + c' \qquad 4.6.36)$$

where c' is another integration constant to be determined. To do this we may use the fact that

$$\varepsilon_2 \left.\frac{d\Psi_2(\zeta)}{d\zeta}\right|_\delta = \zeta_1 \left.\frac{d\Psi_1(\zeta)}{d\zeta}\right|_\delta \qquad 4.6.37)$$

and

$$\left(\frac{\varepsilon_1}{\varepsilon_2}\right)^2 \left(\frac{d\Psi_1(\zeta)}{d\zeta}\right)_\delta^2 = \left(\frac{d\Psi_2(\zeta)}{d\zeta}\right)_\delta^2 = \frac{2D^2}{L_2^2}\cosh[\varphi(\delta)] + c'$$

4.6.38)

so the constant *c'* is determined and one has

$$\left(\frac{d\Psi_2(\zeta)}{d\zeta}\right)^2 = \frac{2D^2}{L_2^2}\left[\cosh[\varphi(\zeta)] - \cosh\left[\frac{1}{2}\Psi_1(\delta)\right] + \frac{L_2^2}{2D^2}\left(\frac{\varepsilon_1}{\varepsilon_2}\right)^2 \left(\frac{d\Psi_1(\zeta)}{d\zeta}\right)_\delta^2\right]$$

$$= \frac{2D^2}{L_2^2}\{\cosh[\varphi(\zeta)] + u\} = b^2\{\cosh[\varphi(\zeta)] + u\}$$

4.6.39)

where $b^2 = \dfrac{2D^2}{L_2^2}$ the remainder u depends (apart on the parameter of the cell) only on $\Psi_1(\delta)$. Now we can write

$$\frac{d\varphi(\zeta)}{d\zeta} = \mp b\sqrt{\cosh[\varphi(\zeta)] + u} \qquad 4.6.40)$$

119

where the upper sign correspond to anodic polarisation and the lower sign to cathodic polarisation. Let us to integrate the previous equation

$$\int_{\varphi(\delta)}^{\varphi(\zeta)} \frac{d\phi}{\sqrt{\cosh\phi + u}} = \mp b\int_{\delta}^{\zeta} d\zeta = \mp b(\zeta - \delta)$$

$$= -\frac{2i\left[F\left(i\varphi(\zeta)/2 \middle| 2/(1+u)\right) - F\left(i\varphi(\delta)/2 \middle| 2/(1+u)\right)\right]}{\sqrt{1+u}}$$

4.6.41)

where $F(\varphi|k) = \int_0^{\varphi} d\phi \sqrt{1 - k\,\mathrm{sen}^2\,\phi}$ is the elliptic integral of the first kind.

Letting $\zeta = 1$, we have

$$\int_{\varphi(\delta)}^{\varphi(1)} \frac{d\phi}{\sqrt{\cosh\phi + u}} = \int_{\frac{\Psi_1(\delta)}{2}}^{-\frac{\Psi_1(\delta)}{2}} \frac{d\phi}{\sqrt{\cosh\phi + u}} = \mp b(1 - \delta)$$

4.6.42)

the left hand side depends on the parameter $\Psi_1(\delta)$ which now can be numerically determined. Then, coming back to the expression 4.6.39 we can

calculate the right hand side of it for a sufficient number of values of φ. We obtain the function $\zeta(\varphi)$ numerically and by reversing the plot this gives us $\varphi(\zeta)$, and therefore $\Psi_2(\zeta)$. This function can be plotted for both anodic and cathodic polarisation. Knowing that $E_2(\zeta) = -\dfrac{kT}{eD}\left[\dfrac{d\Psi_2(\zeta)}{d\zeta}\right]$ is the electric field inside the liquid crystal and that $-\varepsilon_2\varepsilon_0\dfrac{kT}{eD}\left[\dfrac{d^2\Psi_2(\zeta)}{d\zeta^2}\right]$ gives us the total charge density as a function of $\zeta \in [\delta, 1]$ one can plot the electric potential, the electric field and the electric charge.[14]

References.

[1] G. Strangi, D.E. Lucchetta, E. Cazzanelli, N. Scaramuzza, C. Versace and R. Bartolino; *Applied Physics Letters*, **74 (4)**, 534 (1999).

[2] E. Cazzanelli, N. Scaramuzza, G. Strangi, C. Versace, A. Pennisi and F. Simone; *Electrochimica Acta*; **44(18)**, 3101 (1999).

[3] G. Strangi, C. Versace, N. Scaramuzza and V. Bruno; *J. Appl. Phys.*, **92 (7)**, 3630 (2002).

[4] A.L. Alexe-Ionescu, A. Th. Ionescu, N. Scaramuzza, G. Strangi, C. Versace, G.Barbero and R. Bartolino; *Physical Review*, **E 64**, 011708-1 (2001).

[5] G. Strangi, E. Cazzanelli, N. Scaramuzza, C. Versace and R. Bartolino; *Phys. Rev*, **E 62(2)**, 2263 (2000).

[6] V. Bruno, E. Cazzanelli, N. Scaramuzza, G. Strangi, R. Ceccato and G. Carturan; *J. Appl. Phys.* **92 (9),** 5340 (2002).

[7] E. Cazzanelli, S. Marino, V. Bruno, M. Castriota, N. Scaramuzza, G. Strangi, C. Versace, R. Ceccato and G. Carturan; *Solid State Ionics*, **165,** 201 (2003).

[8] S. Marino, M. Castriota, V. Bruno, E. Cazzanelli, G. Strangi, C. Versace, and N. Scaramuzza; "*Electro-Optical investigations of nematic liquid crystal cells containing Titania-Vanadia thin films prepared by sol-gel synthesis*", Submitted to *J. Appl. Phys.*

[9] N. Ozer and C.M. Lampert; *Thin Solid Films*, **349,** 205 (1999).

[10] L.H.M. Krings and W, Talen; *Solar Energy Materials & Solar Cells*, **54,** 27 (1998).

[11] N. Ozer; *Thin Solid Films*, **304,** 310 (1997).

[12] J. Livage, *Chem. Mater*, **3,** 578 (1991).

[13] C. G. Granqvist, Appl. Phys. A: Solids Surf. **57**, 3 (1993)

[14] A. Luiza, A. Ionescu, A. Th. Ionescu, N. Scaramuzza, G. Strangi, C. Versace, G. Barbero, R. Bartolino: Liquid crystal- electrocromic- material interface: A p-n- like electro-optic junction (Physical Review 27 June 2001).

.

.